Modeling gravitational waves from a small mass plunging

Andrea Taracchini

Max Planck Institute for Gravitational Physics (Albert Einstein Institute)
Am Mühlenberg
Potsdam-Golm, 14476, Germany

Alessandra Buonanno

Max Planck Institute for Gravitational Physics (Albert Einstein Institute)
Am Mühlenberg
Potsdam-Golm, 14476, Germany

Gaurav Khanna

Department of Physics
University of Massachusetts Dartmouth
North Dartmouth, MA 02747, USA

Scott A. Hughes

Department of Physics and MIT Kavli Institute
77 Massachusetts Avenue
Cambridge, MA 02139, USA

Gravitational waveforms radiated during the inspiral, plunge and merger stages of a small body moving in the equatorial plane of a Kerr black hole can be exploited to get unique, physical information on the strong-field regime. Such waveforms are constructed by numerically solving the Teukolsky equation in the time domain. When building the source term for the gravitational perturbations, one models the dissipation of orbital energy using the Teukolsky frequency-domain gravitational-wave flux for circular, equatorial orbits, down to the light-ring. The merger features of the Teukolsky waveforms have proven to be instrumental to extending the effective-one-body model of spinning, nonprecessing black-hole binaries, from the comparable-mass to the test-particle limit.

Keywords: Gravitational waves; Kerr metric; black holes; Teukolsky equation; effective-one-body model.

1. Introduction

Gravitational waveforms emitted during the inspiral, plunge and merger stages of a test body orbiting a Kerr black hole have been exploited to grasp unique, physical information on the merger phase and they have been employed to extend analytical models, notably the effective-one-body (EOB) model[1,2], from the comparable-mass to the test-particle limit case[3–12]. Solving the time-domain Regge-Wheeler or Teukolsky equations is significantly less expensive than evolving a black-hole binary in full numerical relativity. The possibility of using the test-particle limit to infer crucial information about the merger waveform of bodies of comparable masses follows from the universality of the merger process throughout the binary parameter space. Some of us[12] investigated the inspiral-merger-ringdown waveforms produced

by the time-domain Teukolsky equation where the source term is evaluated along the quasicircular plunging trajectory of a nonspinning test particle inspiraling in the equatorial plane. The trajectory was computed by solving Hamilton's equations in the Kerr spacetime, augmented by a suitable radiation-reaction force, notably the one constructed from the factorized energy flux of the EOB formalism[13,20]. The Teukolsky waveforms were then used to improve spinning EOB waveforms during the transition from plunge-merger to ringdown. However, that study was limited to moderate spins of the Kerr black hole, i.e., $q \equiv a/M \lesssim 0.8$.

In a later paper[14] we extend the analysis in a few directions. First, in the equations of motion for the orbital dynamics of the plunging particle, we employ the energy flux computed by a highly-accurate frequency-domain Teukolsky code[15,16]. Second, we consider spins in the range $-0.99 \leq q \equiv a/M \leq 0.99$, but investigate in greater detail spins close to extremal.

2. Orbital dynamics to generate inspiral-merger-ringdown Teukolsky waveforms

We model the orbital dynamics using the Hamiltonian of a nonspinning test particle of mass μ in the Kerr spacetime. We numerically solve Hamilton's equations subject to a radiation-reaction force which describes the dissipation of energy into gravitational waves (GWs); the radiation-reaction force is proportional to the sum of the GW energy flux at infinity and through the horizon. We are mainly interested in the characterization of the Teukolsky waveforms, and we want to remove any modeling error from the orbital motion. Similarly to what is done in another paper[17], we source our equations of motion with GW energy fluxes computed in perturbation theory; in particular, we use the Teukolsky fluxes of an earlier work[11], where we numerically solved the Teukolsky equation in frequency domain[15,16] for circular, equatorial orbits all the way down to a radial separation of $r_{\min} = r_{\mathrm{LR}} + 0.01M$, where r_{LR} is the position of the photon orbit.

3. Numerical solution of the time-domain Teukolsky equation

The approach we follow to solve this linear partial differential equation (PDE) is the same as presented in our earlier work[12]. The main points of this technique are as follows: (i) We first rewrite the Teukolsky equation using suitable coordinates — the tortoise radius r^* and Kerr azimuthal angle φ. (ii) Taking advantage of axisymmetry, we separate the dependence on azimuthal coordinate φ. We thus obtain a set of (2+1) dimensional equations. (iii) We recast these equations into a first-order, hyperbolic PDE form. (iv) Finally, we implement a two-step, second-order Lax-Wendroff, time-explicit, finite-difference numerical evolution scheme. The particle-source term on the right-hand-side of the Teukolsky equation requires some care for such a numerical implementation. Two technical advances have been introduced into the solver code aimed at improving results for the present paper.

First, a compactified hyperboloidal layer has been added to the outer portion of the computational domain[18], completely eliminating the "extraction error". Secondly, we have taken advantage of advances made in parallel computing hardware, and we have developed a very high-performing OpenCL implementation of the Teukolsky code that takes full benefit of GPGPU-acceleration and cluster computing[19].

4. Simplicity of inspiral-plunge Teukolsky waveforms for large spins

In the large-spin regime, a prograde inspiraling particle reaches very relativistic speeds before getting to the horizon; for instance, when $q = 0.99$, the peak speed (attained at the peak of the orbital frequency) is around 0.75. At such speeds, the PN expansion is inadequate for analytically describing such systems. However, the Teukolsky inspiral-merger waveforms turn out to be extremely simple. In Fig. 1 we show the amplitudes of the Teukolsky $(2, 2)$ modes for $q = 0.7, 0.8, 0.85, 0.9, 0.95$ aligned at the time when the (ℓ, m) mode reaches its maximum amplitude. We can find a physical explanation for why this happens considering the underlying orbital dynamics. As the spin grows larger, the ISCO moves to smaller separations and gets closer to the horizon, so that the plunging phase becomes shorter (in the radial coordinate), and moves to higher frequencies. This is equivalent to saying that Kerr BHs with larger spins support longer quasicircular inspirals given the same initial frequency. Furthermore, for very large spins the orbital timescale is much shorter than the radiation-reaction timescale. As a result, the secular evolution is much slower for large spins, given the same initial separation.
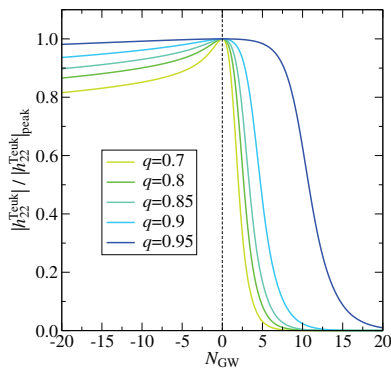

Fig. 1.   Flattening of the peak amplitude of the Teukolsky $(2, 2)$ mode as the spin grows towards 1. The curves are normalized by the values of the amplitude at the peak. We align the waveforms in time at their amplitude peak, and plot them as functions of the number of GW cycles from the peak.

5. Quasinormal-mode mixing in ringdown Teukolsky waveforms

As already found by past numerical investigations of the extreme and small mass-ratio limits, the dominant and leading subdominant ringdown Teukolsky modes can display a rich amplitude and frequency structure that hints at the interference of different QNMs besides the overtones of the least-damped mode, a phenomenon known as mode mixing. In extreme and small mass-ratio binaries, two instances may enhance the excitation and/or mixing of modes other than the (ℓ, m, n)'s in the ringdown of (ℓ, m). On the one hand, for modeling purposes, the strain waveform h is typically decomposed onto -2-spin-weighted spherical harmonics $_{-2}Y_{\ell m}$, while the Teukolsky equation is separated using -2-spin-weighted spheroidal harmonics $_{-2}S_{\ell m}^{q\omega}$, which depend on the Kerr spin q and the (possibly complex) frequency ω of the gravitational perturbation. One finds that the spherical mode $h_{\ell m}$ receives contributions from all spheroidal modes with the same m, but different ℓ. Another source of mixing is the orbital motion of the perturbing particle: whenever $q < 0$, the orbital frequency switches sign during the plunge, because of frame dragging exerted by the spinning BH; this results in a significant excitation of modes with opposite m, but with the same ℓ. We have found that, for $\ell = m$ modes, the QNM mixing is present when $q \leq 0$, and arises mainly due to modes with opposite m, whose excitation grows as the spin decreases. For $\ell \neq m$ modes, instead, we have found QNM mixing across the entire spin range. Fig. 2 shows an example of QNM mixing.
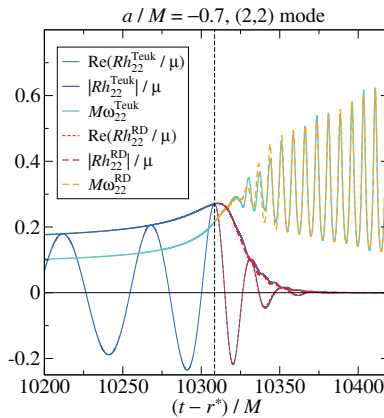

Fig. 2.   Teukolsky $(2, 2)$ mode waveforms for spin -0.7, displaying mode mixing during the ringdown phase: the waveform contains the mode $(2, -2, 0)$ besides the usual $(2, 2, n)$ $(n = 0, 1, \cdots)$ QNMs.

References

1. A. Buonanno and T. Damour, Phys. Rev. D **59**, 084006 (1999) [gr-qc/9811091].
2. A. Buonanno and T. Damour, Phys. Rev. D **62**, 064015 (2000) [gr-qc/0001013].

3. A. Nagar, T. Damour and A. Tartaglia, Class. Quant. Grav. **24**, S109 (2007) [gr-qc/0612096].

4. T. Damour and A. Nagar, Phys. Rev. D **76**, 064028 (2007) [arXiv:0705.2519 [gr-qc]].

5. S. Bernuzzi and A. Nagar, Phys. Rev. D **81**, 084056 (2010) [arXiv:1003.0597 [gr-qc]].

6. S. Bernuzzi, A. Nagar and A. Zenginoglu, Phys. Rev. D **83**, 064010 (2011) [arXiv:1012.2456 [gr-qc]].

7. S. Bernuzzi, A. Nagar and A. Zenginoglu, Phys. Rev. D **84**, 084026 (2011) [arXiv:1107.5402 [gr-qc]].

8. S. Bernuzzi, A. Nagar and A. Zenginoglu, Phys. Rev. D **86**, 104038 (2012) [arXiv:1207.0769 [gr-qc]].

9. A. Taracchini *et al.*, Phys. Rev. D **86**, 024011 (2012) [arXiv:1202.0790 [gr-qc]].

10. T. Damour, A. Nagar and S. Bernuzzi, Phys. Rev. D **87**, no. 8, 084035 (2013) [arXiv:1212.4357 [gr-qc]].

11. A. Taracchini, A. Buonanno, S. A. Hughes and G. Khanna, Phys. Rev. D **88**, 044001 (2013) [Phys. Rev. D **88**, no. 10, 109903 (2013)] [arXiv:1305.2184 [gr-qc]].

12. E. Barausse, A. Buonanno, S. A. Hughes, G. Khanna, S. O'Sullivan and Y. Pan, Phys. Rev. D **85**, 024046 (2012) [arXiv:1110.3081 [gr-qc]].

13. T. Damour, B. R. Iyer and A. Nagar, Phys. Rev. D **79**, 064004 (2009) [arXiv:0811.2069 [gr-qc]].

14. A. Taracchini, A. Buonanno, G. Khanna and S. A. Hughes, Phys. Rev. D **90**, no. 8, 084025 (2014) [arXiv:1404.1819 [gr-qc]].

15. S. A. Hughes, Phys. Rev. D **61**, no. 8, 084004 (2000) [Phys. Rev. D **63**, no. 4, 049902 (2001)] [Phys. Rev. D **65**, no. 6, 069902 (2002)] [Phys. Rev. D **67**, no. 8, 089901 (2003)] [Phys. Rev. D **78**, no. 10, 109902 (2008)] [Phys. Rev. D **90**, no. 10, 109904 (2014)] [gr-qc/9910091].

16. S. Drasco and S. A. Hughes, Phys. Rev. D **73**, no. 2, 024027 (2006) [Phys. Rev. D **88**, no. 10, 109905 (2013)] [Phys. Rev. D **90**, no. 10, 109905 (2014)] [gr-qc/0509101].

17. W. B. Han and Z. Cao, Phys. Rev. D **84**, 044014 (2011) [arXiv:1108.0995 [gr-qc]].

18. A. Zenginoglu and G. Khanna, Phys. Rev. X **1**, 021017 (2011) doi:10.1103/PhysRevX.1.021017 [arXiv:1108.1816 [gr-qc]].

19. J. McKennon, G. Forrester and G. Khanna, arXiv:1206.0270 [gr-qc].

20. Y. Pan, A. Buonanno, R. Fujita, E. Racine and H. Tagoshi, Phys. Rev. D **83**, 064003 (2011) [Phys. Rev. D **87**, no. 10, 109901 (2013)] [arXiv:1006.0431 [gr-qc]].